Calculation of tight binding parameters with density functional theory to describe transport phenomena

Bachelor Thesis

ALBERT-LUDWIGS-
UNIVERSITÄT FREIBURG

Fabian Glatzel

Contents

1 Introduction

1.1 Theoretical Background

1.1.1 Density Functional Theory

The informations of this section are mainly based on [1, 2].
Density functional theory (DFT) is an efficient computational *ab initio* self consistency method to calculate quantum mechanical ground states and it's properties. Since an analytical solution to Schrödinger's equation can only be found in the simplest cases but quantum mechanical effects gain more and more relevance in many fields including nanoelectronics and modern materials sciences, DFT comes in very handy.
A simple look at the many body Schrödinger equation with the electron positions $\vec{r}_i$ and the core positions $\vec{R}_j$

$$\mathcal{H}\Psi\Big(\vec{r}_1, \vec{r}_2, \ldots, \vec{r}_N, \vec{R}_1, \ldots, \vec{R}_M\Big) = E\Psi\Big(\vec{r}_1, \vec{r}_2, \ldots, \vec{r}_N, \vec{R}_1, \ldots, \vec{R}_M\Big) \tag{1.1}$$

shows one of the big problems, since this expression is $3(N+M)$-dimensional. At first the Born-Oppenheimer approximation is applied, stating that the timescale of changing dynamics is for the light electrons much shorter then for the heavy cores and therefore the cores can be assumed fixed at their positions to calculate the electrons ground state, what still leaves a $3N$-dimensional problem.
This is where the Hohenberg-Kohn theorem comes in, which states that the complete electron ground state density

$$n_0(\vec{r}) = N \int \mathrm{d}\vec{r}_2 \cdots \int \mathrm{d}\vec{r}_N |\Psi(\vec{r}, \vec{r}_2, \ldots, \vec{r}_N,)|^2 \tag{1.2}$$

determines the external potential (for example the Coulomb potentials of the cores) and thus the electron ground state wave function Ψ_0. Mathematically this means that the wave function is a unique functional of the electron density with $\Psi_0(\vec{r}) = \Psi[n_0(\vec{r})]$ and consequently every observable can be obtained as a functional of the electron density (this is where the name 'Density Functional Theory' arises).
This includes the energy observable $E[n(\vec{r})]$, which becomes minimal for the correct ground state $n_0(\vec{r})$. Thus the dimension reduces to 3, but leaves a new problem since even if it's known that this functionals exists it contains terms of unknown form due to electron-electron interaction.

To resolve this problem a system with the same electron density out of non directly interacting electrons is assumed. In other words a system of wave functions Φ_i (the so called KOHN-SHAM orbitals) is assumed with:

$$n(\vec{r}) = \sum_i |\Phi_i|^2 \tag{1.3}$$

This wave functions are eigenfunctions to single particle Hamiltonians depending on the electron density $n(\vec{r})$. Again this Hamiltonians contain an unknown term due to many particle interactions, called the *exchange correlation* (XC) term, but can be approximated quite good for most purposes. Thus seperated equations depending on the electron density $n(\vec{r})$ for the single particle wave functions were obtained, which contribute themselve to the electron density $n(\vec{r})$. This equations can be solved by iteration and checking for self consistency.
Through numerical optimization (minimization) of the ground state energy in respect to the core positions it is also possible to find the relaxed them.
To get the band structures the single particle eigenvalues with a constrained periodic behavior according to BLOCHS theorem were calculated (see section 1.1.3).
Finally, calculations with manually shifted charges will be performed using *constrained DFT* (CDFT). This is done by defining i regions containing one or multiple cores with positions $\vec{R}_j$ and an absolute charge N_i for each region. The charge of any region is calculated by integrating the electron density $n(\vec{r})$ multiplied whit a sum of GAUSSIAN curves centred at the atom positions R_j for all cores in the i-th region (see fig. 1.1):

$$w_i(\vec{r}) = \sum_j w\Big(\vec{r} - \vec{R}_j\Big) \tag{1.4}$$

This can be written as minimization problem of the CDFT energy $F[n(\vec{r}), V_i]$:

$$F[n(\vec{r}), V_i] = E_0[n(\vec{r})] + \sum_i V_i \left(\int \mathrm{d}\vec{r}\; w_i(\vec{r})\; n(\vec{r}) - N_i \right) \tag{1.5}$$

with the energy functional of the undisturbed system $E_0[n(\vec{r})]$ and the constraints:

$$0 = \int \mathrm{d}\vec{r}\; w_i(\vec{r})\; n(\vec{r}) - N_i \tag{1.6}$$

for all i regions. The same GAUSSIAN curves are used as external potentials with additional prefactors V_i scaling the strength of the potential to change the density and get the correct charges in each region[1]. The standard deviation σ of the GAUSSIAN curves is left as free parameter. The choice of an appropriate value for σ will be discussed later (see **?? Chapter CDFT for different sigmas**).

[1] In this way the V_i can be understood as LAGRANGE multipliers for the minimization problem of the energy with the constraints of fixed number of charges in the regions

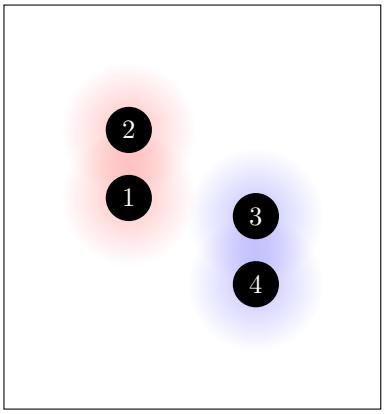

Figure 1.1: Scheme: Sum of GAUSSIAN curves for two regions (red and blue), each with two cores ({1, 2} and {3, 4}), used as weights for the integration/summation over the electron density to calculate the charge in each region.

For the calculations in this thesis the Python DFT package *GPAW* (see [3, 4]) together with the atomic simulation environment *ASE* (see [5]) is used. Especially the *PBE* (named after PERDEW BURKE and ERNZERHOF) XC functional is used, which is a functional of the electron density $n(\vec{r})$ and it's gradient. Further the calculations were performed on a real space grid in the manner of a finite difference method.

1.1.2 Lattice

In the following four sections the informations are basically from [6] if not otherwise noted.
A solid has typically a periodicity in the placing of its atoms. This property is called *crystal structure*, which can be locally restricted due to occurring crystal defects. Exceptions are the amorphous solids, that behave like very viscous fluids and will not be treated here (see [7]).
In the simplest case the atom positions can be described by a BRAVAIS *lattice*. This is a perfectly periodic lattice, where the arrangement and orientation of all atoms look exactly the same from all atom positions (see fig. 1.2a). Therefore the positions $\vec{R}$ of the atoms can be described by:

$$\vec{R} = \sum_{i=0}^{N_D} n_i \vec{a}_i \tag{1.7}$$

with linearly independent primitive vectors $\vec{a}_i$, $n_i \in \mathbb{Z}$ and the dimension N_D.
Often the atom positions do not fulfil this condition but unit cells containing multiple atoms do. Thus additional information about the position of the atoms within the unit cell is needed to characterise the structure. This is called a lattice with a *basis*. An one dimensional example can be seen in fig. 1.2b showing a chain with alternating distances. Here a minimal unit cell (called *primitive cell* or *primitive unit cell*) contains two points and therefore a basis with two basis vectors $\vec{b}_1$ and $\vec{b}_2$. The primitive cell itself fulfils the condition of a Bravais lattice with

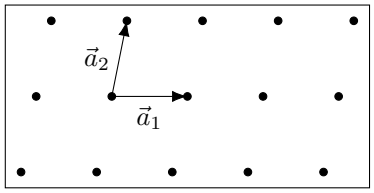

(a) Two dimensional BRAVAIS lattice with primitive vectors $\vec{a}_1$ and $\vec{a}_2$

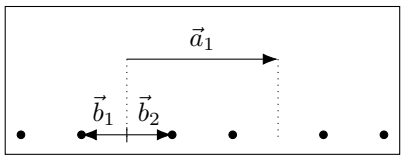

(b) One dimensional BRAVAIS lattice with a basis $\{\vec{b}_1, \vec{b}_2\}$

Figure 1.2: Schemes of BRAVAIS *lattices*

primitive vector $\vec{a}_1$. If there were no alternation in the chain and all points were equally spaced, the points would form a Bravais lattice themselves with a primitive vector of half the length of $\vec{a}_1$. This will be of importance later in section 1.1.5.
It should be mentioned that a primitive call can always be constructed by simply taking all space closer to a certain lattice point then to all others. This kind of primitive cells are called WIGNER-SEITZ *primitive cells.*
The set of wave vectors $\vec{K}$, that have the periodicity of a given BRAVAIS lattice $\vec{R}$, explicitly:

$$\exp\left(\mathrm{i}\vec{K}\cdot\vec{r}\right) = \exp\left[\mathrm{i}\vec{K}\cdot\left(\vec{r}+\vec{R}\right)\right] \qquad \Leftrightarrow \qquad \vec{K}\cdot\vec{R} = \mathbb{Z}\cdot 2\pi \tag{1.8}$$

do also form a BRAVAIS lattice in the reciprocal space, the so called *reciprocal lattice.* The WIGNER-SEITZ primitive cell of the reciprocal lattice, namely the *First* BRILLOUINE *Zone*, will be relevant for the next section.

1.1.3 Bloch Theorem

According to BLOCH'S theorem a wave function $\Psi(\vec{r})$ of a periodic potential, $V\left(\vec{r}+\vec{R}\right) = V\left(\vec{r}\right)$ for all $\vec{R}$ of a BRAVAIS lattice, can be written in the form:

$$\Psi(\vec{r}) = \exp\left(\mathrm{i}\vec{k}\cdot\vec{r}\right)\cdot u(\vec{r}) \tag{1.9}$$

where $\vec{k}$ is an arbitrary wave vector and $u(\vec{r})$ denotes a $\vec{R}$-periodic function.
Under the assumption, that the boundary condition at the surface should not change the physical properties of the bulk, one assumes the periodic BORN-VON KARMAN *boundary condition*[2]:

$$\Psi(\vec{r}+N_i\vec{a}_i) = \Psi(\vec{r}) \tag{1.10}$$

[2] Alternatively one can choose the boundary condition for a vanishing wave function on the surface $\Psi\left(\vec{S}\right) = 0$. But the periodic boundary condition has the advantage, that it corresponds with propagating waves, which suite transport phenomena very well, whereas a vanishing boundary condition corresponds with standing waves.

where N_i denotes the number of unit cells in the direction $\vec{a}_i$ of the bulk. Hereby one obtains an additional condition for the wave vectors $\vec{k}$, namely:

$$\vec{k} = \sum_{i=1}^{N_D} \frac{m_i}{N_i} \vec{b}_i \qquad m_i \in \mathbb{Z} \tag{1.11}$$

It can be shown that if two states only vary in the way that $\vec{k}_1 - \vec{k}_2 \in \vec{K}$, they correspond to the same physical state. From this can be concluded, that one has to take only the states within the first BRILLOUINE zone into account for a complete description. One considers that the number of states in the first BRILLOUINE zone equals the number of sites $N = \prod_{i=1}^{N_D} N_i$ of the bulk. For the one dimensional case this means, that the number of states within the first BRILLOUINE zone is the number of primitive cells in the chain.
Since there are multiple solutions to SCHRÖDINGER'S equation for a given $\vec{k}$, they will be labeled by some additional index n. In solid state physics the number of atoms contained in a system is usually very big, what corresponds to a high density of states in the reciprocal space. As limit a continuum of states can be assumed in the reciprocal space, which leads to a continuum of eigenenergies in some interval (*band*), since the SCHRÖDINGER equation changes continuous with $\vec{k}$. Therefore n is referred to as *band index*. Two bands of special interest are the *HOMO*-band (referring to the 'highest occupied molecular orbital') and the *LUMO*-band (referring to the 'lowest unoccupied molecular orbital').

1.1.4 Tight-Binding Method

In the previous section the eigenstates have been calculated by using the translational symmetries of a BRAVAIS lattice, which results in completely delocalized states. A complete different approach is the following:
If the distance between adjacent atoms is much bigger than the typical width of the electron wave functions for isolated atoms, the wave functions shouldn't differ much from that states. Decreases the distance between the atoms, the electrons will start to feel the presence of the other atoms and will therefore change their states. The tight-binding method handles the case in which the interaction doesn't completely change the wave functions, but the effects are to big to neglect. Since the tight-binding method is a single particle model, it seems quite suitable for the KOHN-SHAM orbitals and therefore for the description of the band structures.
Mathematically one starts with the basic single atom Hamiltonian $\mathcal{H}_{\text{at}}$ and it's single particle eigenfunctions φ_n satisfying the Schrödinger equation of an isolated atom:

$$\mathcal{H}_{\text{at}} \varphi_n = E_n \varphi_n \tag{1.12}$$

In the next step a second term is added to the Hamiltonian, that applies the corrections needed to describe the lattice correctly. In an one dimensional chain with atom positions $\vec{R}_i$ the modified

Hamiltonian contains a term describing the interaction U of adjacent valence electrons with the matrix elements $M_{i,i\pm1}$:

$$M_{i,i\pm1} = \int \mathrm{d}\vec{r}\; \varphi_n^*\Big(\vec{r} - \vec{R}_i\Big)\; U\; \varphi_n\Big(\vec{r} - \vec{R}_{i\pm1}\Big) \tag{1.13}$$

In can be shown that this term is negative if the wave functions have the same sign where they meet and therefore form a binding state (see [8]). Hence the positive so called *hopping parameter* $t_{i,i\pm1} = -M_{i,i\pm1}$ is introduced. In terms of second quantization this interaction Hamiltonian can be written as[3]:

$$-\sum_i t_{i,i+1}\Big(c_i^\dagger\; c_{i+1} + c_{i+1}^\dagger\; c_i\Big) \tag{1.14}$$

with the creation and annihilation operators $c_i^\dagger, c_i$ for an electron located at the i-th atom. Thus the term $c_i^\dagger c_{i\pm1}$ can be interpreted as shifting an electron from the $(i \pm 1)$-th atom to the i-th atom which explains the name hopping parameter for t.
The combination of the single atom Hamiltonian $\mathcal{H}_{\mathrm{at}}$ and the next-neighbor-hopping term in the basis of the single atom wave functions φ_n for the i atoms can than be written as:

$$\mathcal{H} = \sum_i E_n n_i - \sum_i t_{i,i+1}\Big(c_i^\dagger\; c_{i+1} + c_{i+1}^\dagger\; c_i\Big) \tag{1.15}$$

with the number operator $n_i = c_i^\dagger c_i$, that simply returns the number of electrons in the state φ_n of the i-th atom. In matrix notation this Hamiltonian would look like:

$$\mathcal{H} = \begin{pmatrix} \ddots & & & & \\ & E_n & -t_{i-1,i} & 0 & \\ & -t_{i,i-1} & E_n & -t_{i,i+1} & \\ & 0 & -t_{i+1,i} & E_n & \\ & & & & \ddots \end{pmatrix} \tag{1.16}$$

In the simple case of equally spaced atoms with distance a all hopping parameters become the same $t_{i,i\pm1} = t \quad \forall i$.

1.1.5 Peierls Distortion and SSH-Hamiltonian

Peierls instability theorem states, that an one-dimensional chain of atoms with a single unpaired electron will always distort from an perfect periodic placing of its atoms (see [9, 10]). Or in other words, breaking the symmetry under the previous told conditions will lower the ground state energy.

[3] neglecting spin degree of freedom

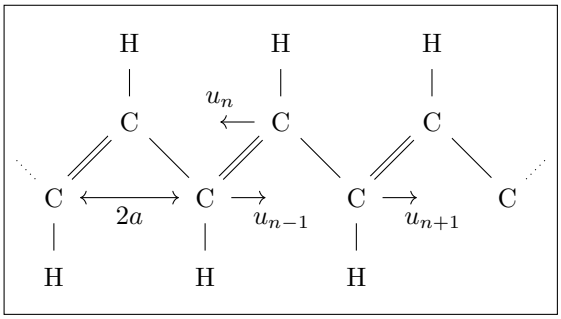

Figure 1.3: Structural formula of *trans*-polyacetylene

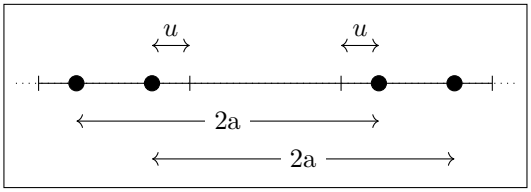

Figure 1.4: Scheme: perfectly dimerized molecule

Thus a displacement u_n of the atoms is expected yielding the new atom positions:

$$R_n \mapsto (-1)^n u_n + R_n \tag{1.17}$$

As a consequence also the hopping-parameter will be effected in the way $t_{n,n+1} = t_0 + \delta_n$ and for small displacements u_n the linear approximation $\delta_n = \alpha(u_{n+1} - u_n)$ with the *phonon coupling constant* $\alpha = {}^{\partial t}/_{\partial u_n}$ will hold.
An important example which includes this hopping-term is the Hamiltonian used to describe the electron-hopping in *trans*-polyacetylene (see fig. 1.3). Here u_n describes the displacement of an CH group.

Assuming that the σ-binding energy can be expanded to second order about the symmetric state using an effective spring constant κ the energy contribution can be written as:

$$\frac{\kappa}{2} \sum_n (u_{n+1} - u_n)^2 \tag{1.18}$$

The π-binding energy is described in the tight-binding approximation derived earlier[4]. Finally the term of the kinetic energy of the atoms is added to get the so called *SSH-Hamiltonian* (named after W. P. Su, J. R. Schrieffer, A. J. Heeger, see [11, 12]):

$$\mathcal{H}_{\text{SSH}} = \underbrace{-2 \sum_n t_{n+1,n} \left(c_{n+1}^\dagger c_n + c_n^\dagger c_{n+1} \right)}_{\text{electron hopping / } \pi\text{-binding energy}} + \underbrace{\frac{1}{2} \sum_n \kappa (u_{n+1} - u_n)^2}_{\sigma\text{−binding energy}} + \underbrace{\frac{1}{2} \sum_n M \dot{u}_n^2}_{\text{kinetic energy}} \tag{1.19}$$

[4] since the description is spinless an additional factor 2 is obtained

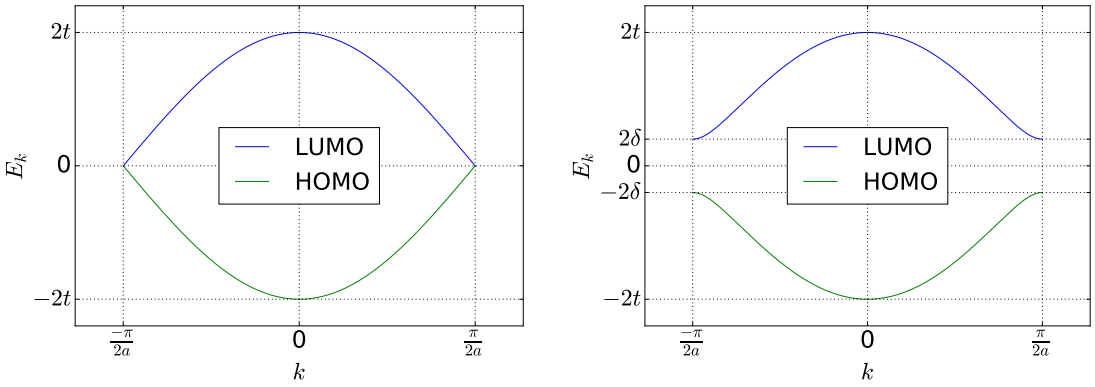

(a) Band structure for no distortion ($u = 0$) leading to no band gap

(b) Band structure for distortion ($u \neq 0$) leading to a band gap of 4δ

Figure 1.5: Structure of the HOMO- and LUMO-band arising from a tight-binding treatment of next-neighbor-hopping

Using Born-Oppenheimer approximation and a perfect symmetric dimerization $u_n = (-1)^n u$ (see fig. 1.4) the Hamiltonian can be written as:

$$\mathcal{H} = -2\sum_n [t_0 + (-1)^n \delta] \cdot \left(c_{n+1}^\dagger c_n + c_n^\dagger c_{n+1}\right) + 2N\kappa u^2 \tag{1.20}$$

$$= -2\sum_n^{N_d} \left[(t_0+\delta)\left(c_{2n+1}^\dagger c_{2n} + c_{2n}^\dagger c_{2n+1}\right) + (t_0-\delta)\left(c_{2n}^\dagger c_{2n-1} + c_{2n-1}^\dagger c_{2n}\right)\right] + 2N\kappa u^2 \tag{1.21}$$

Calculation of the k-space representations of the creation and annihilation operators finally leads to the expression:

$$\mathcal{H} = \sum_k \left[(\epsilon_k + i\Delta_k) c_k^{\dagger(e)} c_k^{(o)} + (\epsilon_k - i\Delta_k) c_k^{\dagger(o)} c_k^{(e)}\right] + 2N\kappa u^2 \tag{1.22}$$

with the substitutions $\epsilon_k := 2t_0 \cos(ka)$ and $\Delta_k := 2\delta \sin(ka)$. Here $c_k^{\dagger(e)}$, $c_k^{\dagger(o)}$, $c_k^{(e)}$, $c_k^{(o)}$ are the creation and annihilation operators at the even/odd $(e)/(o)$ positions to a certain k-point. Due to the displacement the primitive cell length doubled and therefore the first Brillouine zone goes only from $^{-\pi}/_{2a}$ to $^{\pi}/_{2a}$.
In further calculations the term $2N\kappa u^2$ will be neglected since it's only causing an offset. Thus the contribution of the Hamiltonian responsible for the form of th band structure is given by the terms:

$$\mathcal{H}_k = [\epsilon_k + i\Delta_k] c_k^{\dagger(e)} c_k^{(o)} + [\epsilon_k - i\Delta_k] c_k^{\dagger(o)} c_k^{(e)} \tag{1.23}$$

with the eigenvalues (see fig. 1.5):

$$E_k = \pm\sqrt{\epsilon_k^2 + \Delta_k^2} \tag{1.24}$$

and the eigenstates:

$$\Psi_k^{(c)} = \frac{1}{\sqrt{2}}\left(c_k^{\dagger(e)} + \frac{\epsilon_k - i\Delta_k}{|E_k|}c_k^{\dagger(o)}\right) \tag{1.25}$$

$$\Psi_k^{(v)} = \frac{1}{\sqrt{2}}\left(c_k^{\dagger(e)} - \frac{\epsilon_k - i\Delta_k}{|E_k|}c_k^{\dagger(o)}\right) \tag{1.26}$$

corresponding to the valance (v) and conduction (c) band. Hereby the eigenfunctions have to be understood as operating on the vacuum state, $|(e),(o)\rangle = |0,0\rangle$. Thus the following relations can easily be shown:

$$\left\langle \Psi_k^{(\lambda)} \middle| \Psi_k^{(\lambda\prime)} \right\rangle = \delta_{\lambda,\lambda\prime} \tag{1.27}$$

$$\left\langle \Psi_k^{(v)} \middle| \mathcal{H}_k \middle| \Psi_k^{(v)} \right\rangle = -|E_k| \tag{1.28}$$

$$\left\langle \Psi_k^{(c)} \middle| \mathcal{H}_k \middle| \Psi_k^{(c)} \right\rangle = |E_k| \tag{1.29}$$

It should be mentioned, that these E_k are eigenvalues to single particle Hamiltonians. As a consequence the sum over all band structure energies of occupied states isn't equal to the ground state energy. For example the Coulomb repulsion of the electrons would be added twice and other terms of the exchange correlation energy would be left out. Nevertheless the sum over the HOMO-band energies is some quantity worth to compare:

$$E_0(u) = -2\sum_k |E_k| \tag{1.30}$$

$$= \frac{-4Nt_0}{\pi} \underbrace{\int_0^{\pi/2} \mathrm{d}\theta \sqrt{1 - \left(1 - \frac{\delta^2}{t_0^2}\right)\sin^2(\theta)}}_{=:F(\delta/t_0)} \tag{1.31}$$

For small δ/t_0 the integral is approximately 1.

2 Results

The predictions of the previous sections are tested on *trans*-polyacetylene. Therefore the convergence is checked first. Since *trans*-polyacetylene has an alternation of single and double bonds between the carbon atoms, a unit cell containing two CH-groups with periodic boundary conditions in one dimension is used (see fig. 2.1).

2.1 Convergence Testing of Polyacetylene

To check the convergence in respect to a certain parameter, all other parameters are chosen in a way, that the energy is definitely converged in respect to them. This includes also a relaxation of the atom positions in each step.
First the convergence of the ground state energy in respect to the number of used k- points is tested, whereat automatic Brillouin zone sampling is used. It can be seen, that the energy is quite good converged for approximately 15 k-points (see fig. 2.2), since a comparison of the energies for 15 and 100 k-points leads to a difference of only 0.014 eV.

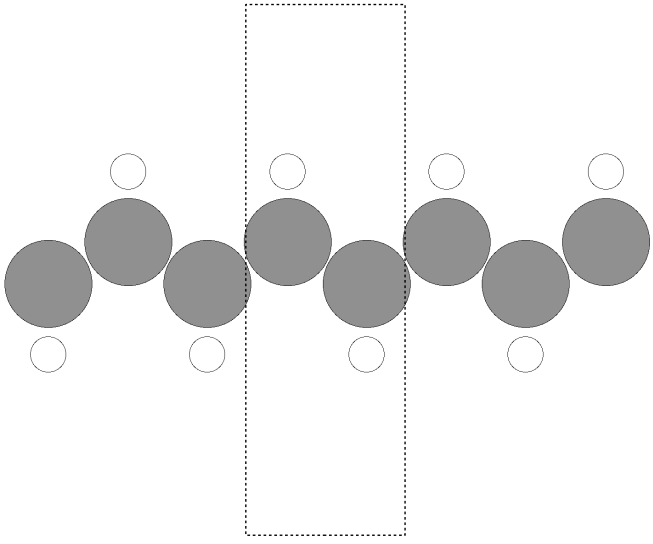

Figure 2.1: Scheme: Unit cell for *trans*-polyacetylene with periodic boundary conditions in one dimension. The grey circles represent the carbon atoms, the white ones the hydrogen atoms.

In fig. 2.3 the ground state energy in respect to the grid spacing can be seen. Since the number of grid points grows with $1/h^3$, it is very important to find a reasonable compromise between computing time and accuracy. Because our system isn't that big, a h value of 0.1 Å is used for further calculations.
The lowering of the ground state energy in respect to the maximum force for the relaxation process of the cores is in comparison with previous dependencies small. Therefore a maximum force of 0.1 eV/Å should be appropriate.
Finally the convergence of the energy in respect to the unit cell width (not in the direction of the periodic boundary condition) is tested. As can be seen in fig. 2.5, the ground state energy increases for small unit cell widths, what can be understood intuitively by comparison to the quantum mechanical 'particle in a box'. For a with of approximately 9 Å a stable level is reached, what corresponds with a minimal distance between cores and cell surface of approximately 3 Å (same for second direction of non periodic boundaries).
Convergence testing for other systems is done analogously and thus is added to the appendix.

2.2 Physical Quantities of Polyacetylene

First, the bond length in direction of the periodic boundaries a is calculated (see fig. 1.3). This quantity corresponds with the half unit cell length in direction and thus is calculated by minimizing the ground state energy in respect to the cell length (see fig. 2.6). Through a quadratic fit a parameter of $a = 1.23$ Å is obtained, what matches a literature value of 1.2 Å (from [13]) perfectly.
Second, the displacement u of the carbon atoms is checked. Here no distortion at all is obtained ($u < 10^{-4}$ Å) by using automatic k-point sampling, which doesn't include a k-point directly at the edge of the Brillouin zone. If the k-points are chosen manually in the way, that a k-point at the edge of the Brillouin zone is included, a bigger displacement of approximately $u = 5 \cdot 10^{-3}$ Å is obtained (see fig. 2.7). In comparison to a literature value of $u = 0.042$ Å (from [13, 14]) it is still one order of magnitude to small, but it is known, that PBE delocalizes electrons to much, which results in to small distortions and therefore in to small band gaps (see [15, 16]).
The importance of the k-point at the edge of the Brillouin zone can be understood by looking at the sign of the p-orbitals of carbon, which form an alternating π bond (see fig. 2.8). Consequently the gamma point is expected to be important for getting asymmetry in an unit cell containing four carbon atoms. This is checked by simply using automatic k-point sampling, which includes the gamma point for an odd number of k-points automatically. As expected an alternating behaviour for the displacement in respect to the number of k-points can be seen in fig. 2.9.

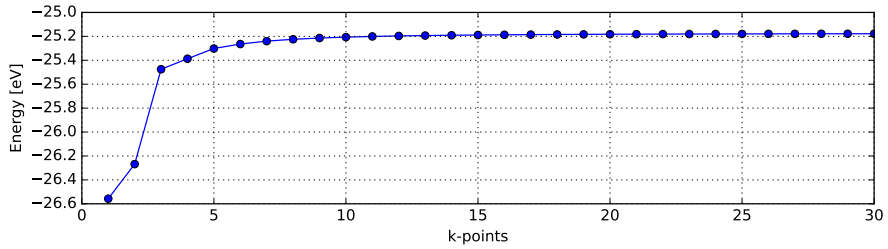

Figure 2.2: Ground state energy of relaxed polyacetylene in respect to the number of k-points

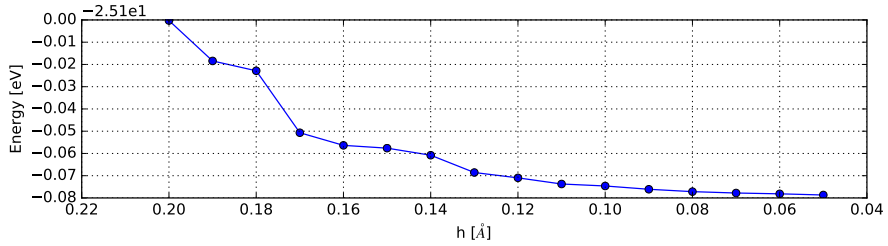

Figure 2.3: Ground state energy of relaxed polyacetylene in respect to the grid spacing

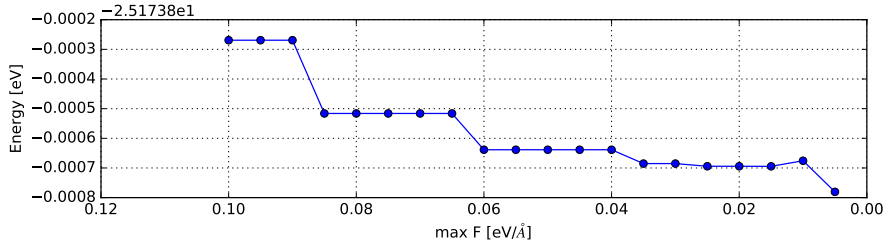

Figure 2.4: Ground state energy of relaxed polyacetylene in respect to the maximum force, for which the relaxation process stops

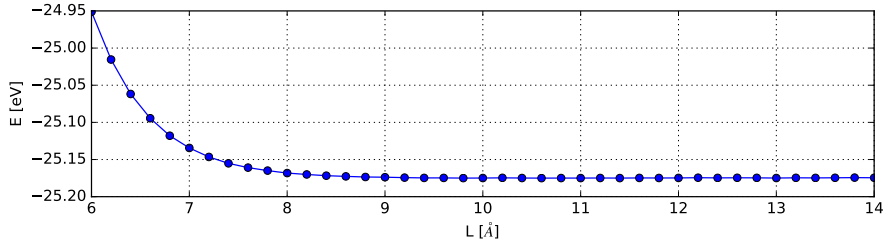

Figure 2.5: Ground state energy of relaxed polyacetylene in respect to the width of the unit cell (not in direction of periodic boundary condition)

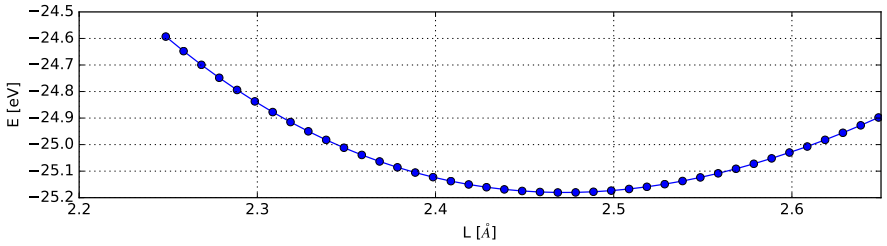

Figure 2.6: Ground state energy or relaxed polyacetylene in respect to the length of the unit cell in direction of periodic boundaries

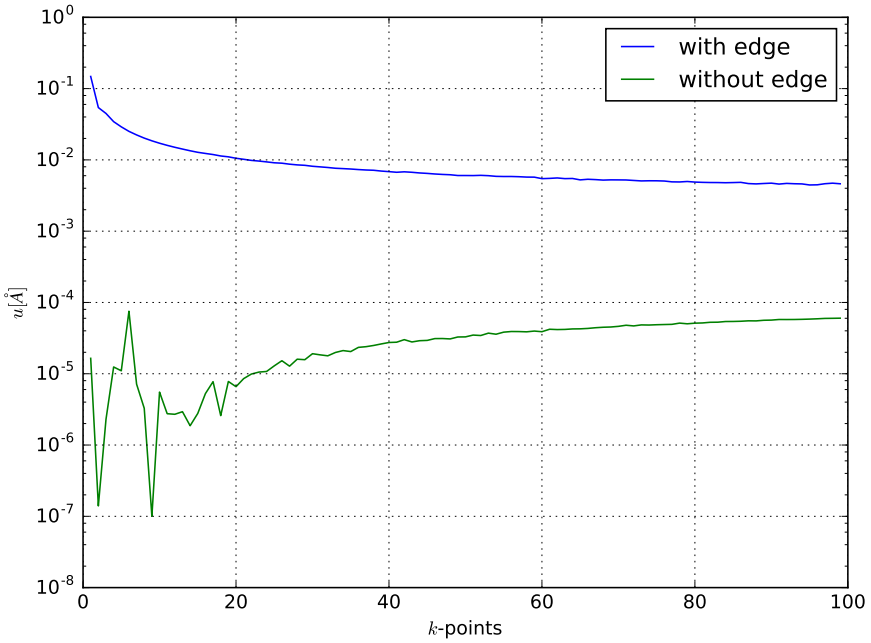

Figure 2.7: Displacement u of the carbon atoms in respect to the number of k-points for automatic sampling (without k-point at the edge of the Brillouin zone) and manually placed k-points (with one k-point at the edge of the Brillouin zone).

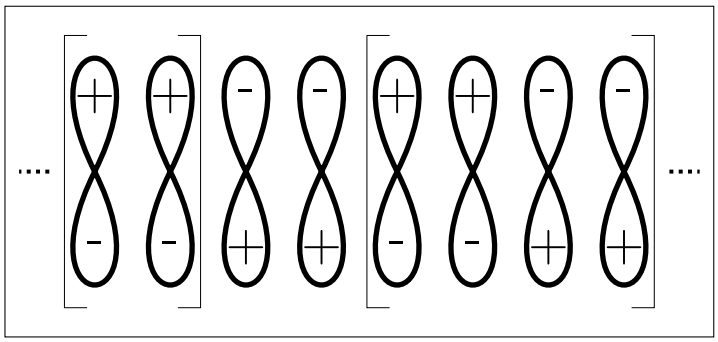

Figure 2.8: Scheme: Sign of p-orbitals in a linear chain, that form an alternating π bond. The phase difference of two adjacent unit cells, which contain two carbon atoms, is given by π, whereas the phase difference of two adjacent unit cells, each with four carbon cores, is given by zero.

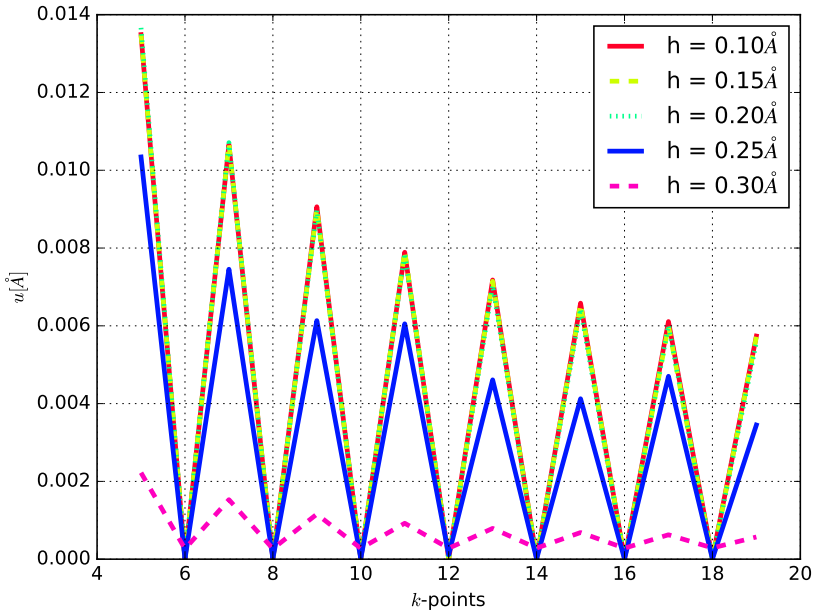

Figure 2.9: Displacement u of the carbon atoms in respect to the number of k-points for automatic sampling and different grid spacings h. The gamma point is automatically included for odd numbers of k-points, which leads to some asymmetry.

2.3 Real Stuff

In the following plots the k-point values are always given relative to the basis vectors of the reciprocal unit cell. Thus a value of $k = \pm 0.5$ corresponds to a state at the edge of the Brillouin zone.

3 Chaos

To model the charging applied with CDFT of the two regions with $\pm q$ two approaches will be tested:

1) simple modifications of the wave functions under the assumption that all k-points contribute equally to the charge displacement
2) modification of the Hamiltonian describing the external potential for the different regions

The first approach leads to the valence wave function:

$$\Psi_k^{(v)}(q) = \sqrt{\frac{1}{2} - \frac{q}{2}}\, c_k^{\dagger(e)} - \sqrt{\frac{1}{2} + \frac{q}{2}}\, \frac{\epsilon_k - i\Delta_k}{|E_k|} c_k^{\dagger(o)} \tag{3.1}$$

with the following expectation values for the energies:

$$\left\langle \Psi_k^{(v)}(q) \middle| \mathcal{H}_k \middle| \Psi_k^{(v)}(q) \right\rangle = -\sqrt{1-q^2}\,|E_k| \tag{3.2}$$

And the sum over the HOMO-band energies:

$$E_0(q) = -\frac{4Nt_0}{\pi}\sqrt{1-q^2} \tag{3.3}$$

The second approach leads to the Hamiltonian which decreases/increases the energies at the even/odd positions:

$$\mathcal{H}_k = [\epsilon_k + i\Delta_k] c_k^{\dagger(e)} c_k^{(o)} + [\epsilon_k - i\Delta_k] c_k^{\dagger(o)} c_k^{(e)} - V n_k^{(e)} + V n_k^{(o)} \tag{3.4}$$

or in matrix notation:

$$\mathcal{H}_k = \begin{pmatrix} -V & \epsilon_k + i\Delta_k \\ \epsilon_k - i\Delta_k & V \end{pmatrix} \tag{3.5}$$

with the eigenvalues $E_k = \pm\sqrt{V^2 + \epsilon_k^2 + \Delta_k^2}$ and the eigenstates[1]:

$$\vec{\Psi}_k(V) = \left[2\left(E_k^2 \mp V|E_k|\right)\right]^{-1/2} \cdot \begin{pmatrix} -V \pm \sqrt{V^2 + \epsilon_k^2 + \Delta_k^2} \\ \epsilon_k - i\Delta_k \end{pmatrix} \tag{3.6}$$

[1] the valence state corresponds with the lower signs

For $V = 0$ this matches the previous result. The sum over the HOMO-band energies becomes approximately:

$$E_0 = \frac{-2N}{\pi}\sqrt{V^2 + 4t_0^2} \tag{3.7}$$

Since a bigger absolute of the displaced charge $|q|$ is expected for a bigger absolute of the external potential $|V|$ these two approaches contradict each other (compare eqs. (3.3) and (3.7)).

3.1 Other Preparations

3.2 Hydrogen Chain

A simple system of equidistant hydrogen atoms is used to test the predictions of the earlier motivated Hamiltonian. For this purpose the set-up and convergence of the unit cell will be tested. Afterwards the results from the application of CDFT to the band structure will be shown and compared to the predictions of our modeling approaches.

3.2.1 Unit Cell Set-Up

Even if there's no distortion, a unit cell with two hydrogen atoms is needed, because later the application of the external potential and the consequential charge displacement will break the symmetry. All calculations for hydrogen will be performed using spin polarization, since this lowers the ground state energy and later this will be essential for the convergence of the wave functions (**WRONG**) in the presence of the external potentials. Therefore it's necessary for the optimizer to break the symmetry by setting the initial magnetic moments of the atoms to $\pm 1/2$.

3.2.2 Results

First of all the HOMO band shows the expected $E(k) \propto -\cos(ka)$ behaviour (see fig. 3.1). Through fitting to the HOMO band the hopping parameter $t_0 = 4.78\,\mathrm{eV}$ can be obtained.
In the next step the band structures for the periodically charged hydrogen atoms will be calculated (see fig. 3.2). As expected from the symmetry the band structures do not depend on the direction (sign) of the charge displacement. It can also be seen, that the influence of charging is bigger for k-points closer to the edge of the Brillouin zone and the bands become shifted to lower energies. Both is in good agreement with the predictions of the Hamiltonian.
In fig. 3.3 the height of the Gaussian potentials causing the charge displacement as a function of the transferred charge is shown. Again the symmetry is as expected and in the region of $-0.2 \leq q \leq 0.2$ the dependency is approximately linear.
From the model Hamiltonian the state energy at the edge of the Brillouin zone ($k \cdot a = \pi/2$) is expected to have the form $E_{\mathrm{edge}} = -\sqrt{V^2} = -\sqrt{c^2 \cdot U_{\mathrm{CDFT}}^2}$. As can be seen in fig. 3.4 this

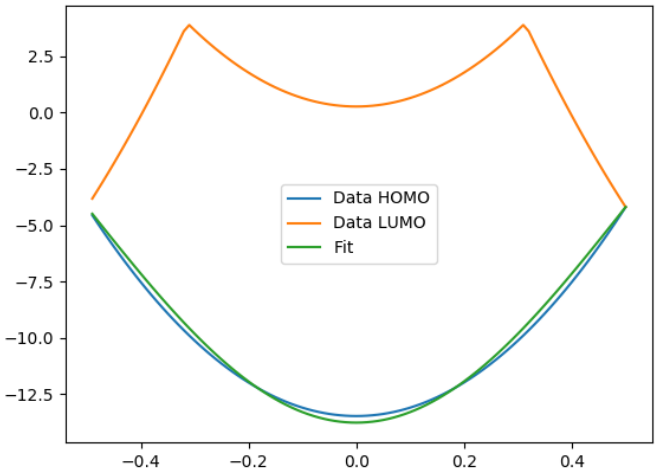

Figure 3.1: $E(k)$

matches the results of the simulation very well. From a fit to this data the ratio between the theoretical potential and the voltage from CDFT can be obtained: $V \approx 13.265\,\mathrm{e} \cdot U_{\mathrm{CDFT}}$. Analogously this ratio can be calculated by fitting the energy at the gamma point to $E_{\mathrm{gamma}} = -\sqrt{c^2 \cdot U_{\mathrm{CDFT}}^2 + 4 \cdot t_0^2}$ (see fig. 3.5). Here the proportionality constant becomes $V \approx 11.289\,\mathrm{e} \cdot U_{\mathrm{CDFT}}$, which corresponds to a relative difference of approximately 20%. To take a closer look at this effect the proportionality constant is calculated by fitting for many different k-points (see fig. 3.6).

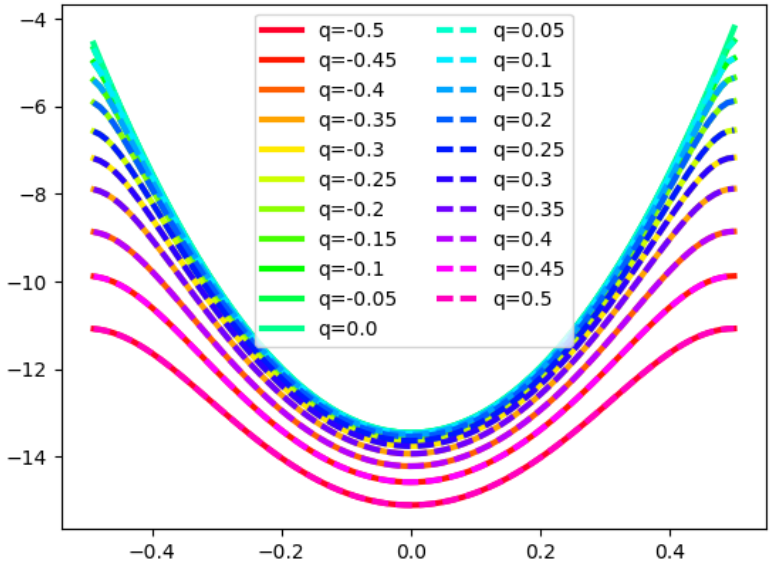

Figure 3.2: $E(k, q)$

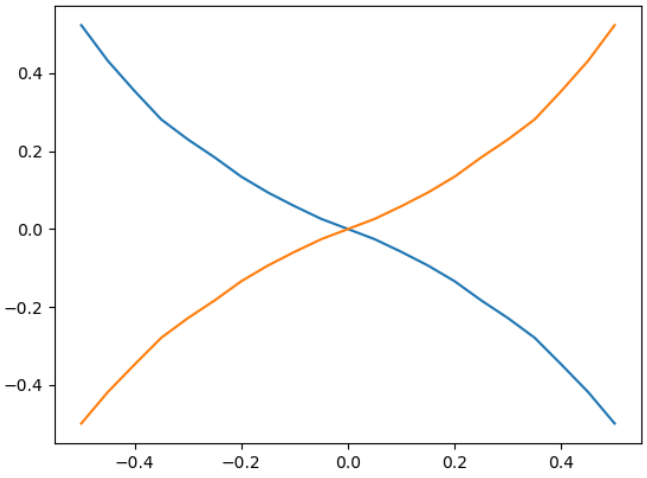

Figure 3.3: $V(q)$

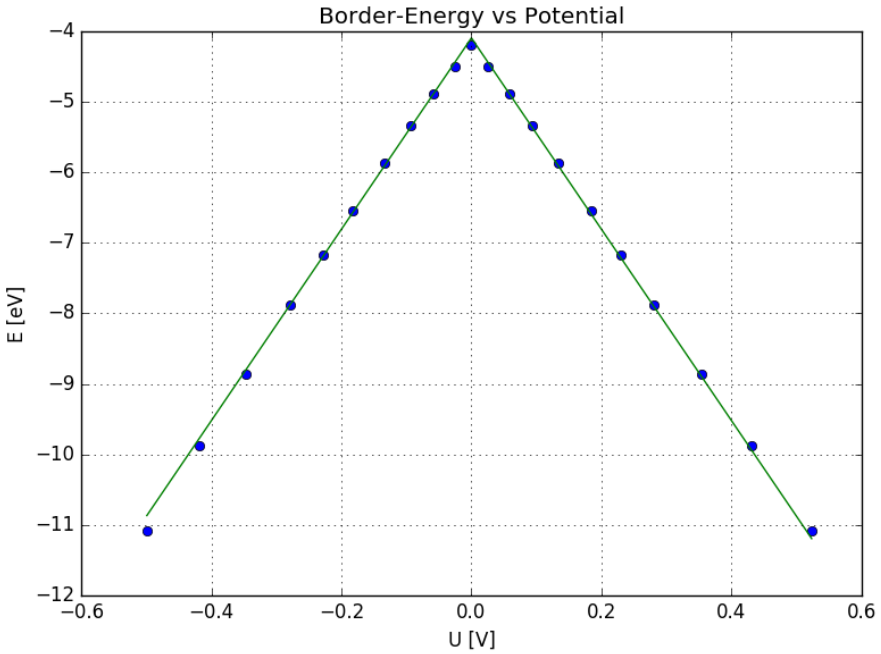

Figure 3.4: $E(U)$

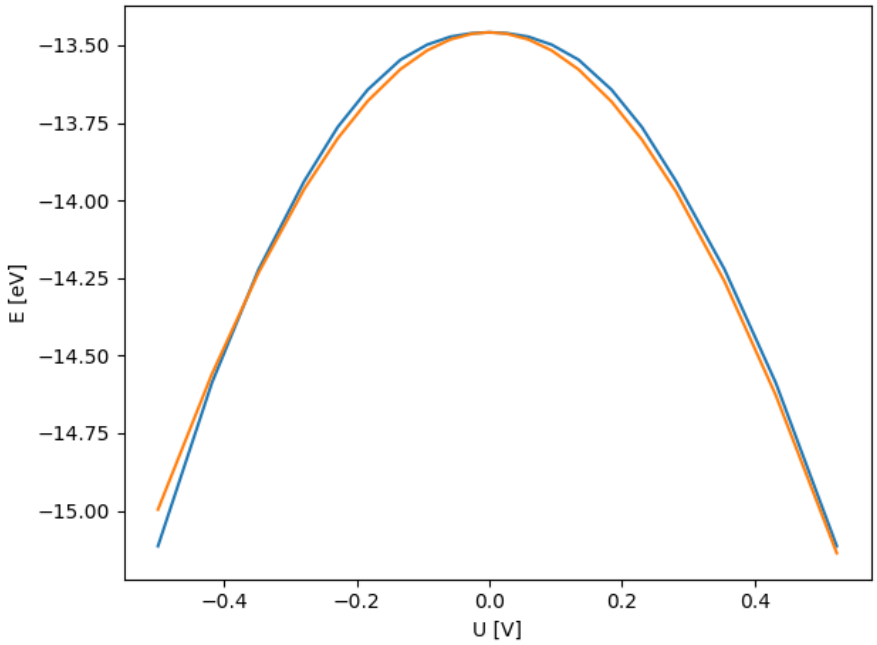

Figure 3.5: $E(U)$

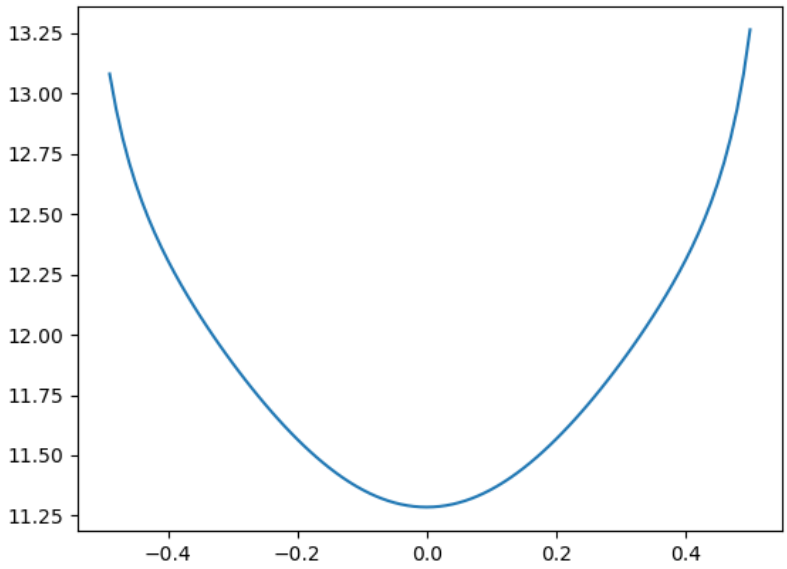

Figure 3.6: $c(k)$

List of Figures

List of Tables

Bibliography

[1] Koskinen, Pekka ; Mäkinen, Ville: Density-functional tight-binding for beginners. In: *Computational Materials Science* 47 (2009), Nr. 1, 237 - 253. http://dx.doi.org/http://dx.doi.org/10.1016/j.commatsci.2009.07.013. – DOI http://dx.doi.org/10.1016/j.commatsci.2009.07.013. – ISSN 0927–0256

[2] Barth, U von: Basic Density-Functional Theory—an Overview. In: *Physica Scripta* 2004 (2004), Nr. T109, 9. http://stacks.iop.org/1402-4896/2004/i=T109/a=001

[3] Mortensen, J. J. ; Hansen, L. B. ; Jacobsen, K. W.: Real-space grid implementation of the projector augmented wave method. In: *Phys. Rev. B* 71 (2005), JAN, Nr. 3, S. 035109. http://dx.doi.org/10.1103/PhysRevB.71.035109. – DOI 10.1103/PhysRevB.71.035109. – ISSN 1098–0121

[4] Enkovaara, J ; Rostgaard, C ; Mortensen, J J. ; Chen, J ; Dułak, M ; Ferrighi, L ; Gavnholt, J ; Glinsvad, C ; Haikola, V ; Hansen, H A. ; Kristoffersen, H H. ; Kuisma, M ; Larsen, A H. ; Lehtovaara, L ; Ljungberg, M ; Lopez-Acevedo, O ; Moses, P G. ; Ojanen, J ; Olsen, T ; Petzold, V ; Romero, N A. ; Stausholm-Møller, J ; Strange, M ; Tritsaris, G A. ; Vanin, M ; Walter, M ; Hammer, B ; Häkkinen, H ; Madsen, G K H. ; Nieminen, R M. ; Nørskov, J K. ; Puska, M ; Rantala, T T. ; Schiøtz, J ; Thygesen, K S. ; Jacobsen, K W.: Electronic structure calculations with GPAW: a real-space implementation of the projector augmented-wave method. In: *Journal of Physics: Condensed Matter* 22 (2010), Nr. 25, 253202. http://stacks.iop.org/0953-8984/22/i=25/a=253202

[5] Larsen, Ask H. ; Mortensen, Jens J. ; Blomqvist, Jakob ; Castelli, Ivano E. ; Christensen, Rune ; Dułak, Marcin ; Friis, Jesper ; Groves, Michael N. ; Hammer, Bjørk ; Hargus, Cory ; Hermes, Eric D. ; Jennings, Paul C. ; Jensen, Peter B. ; Kermode, James ; Kitchin, John R. ; Kolsbjerg, Esben L. ; Kubal, Joseph ; Kaasbjerg, Kristen ; Lysgaard, Steen ; Maronsson, Jón B. ; Maxson, Tristan ; Olsen, Thomas ; Pastewka, Lars ; Peterson, Andrew ; Rostgaard, Carsten ; Schiøtz, Jakob ; Schütt, Ole ; Strange, Mikkel ; Thygesen, Kristian S. ; Vegge, Tejs ; Vilhelmsen, Lasse ; Walter, Michael ; Zeng, Zhenhua ; Jacobsen, Karsten W.: The atomic simulation environment—a Python library for working with atoms. In: *Journal of Physics: Condensed Matter* 29 (2017), Nr. 27, 273002. http://stacks.iop.org/0953-8984/29/i=27/a=273002

[6] Ashcroft, N.W. ; Mermin, N.D.: *Solid State Physics*. Holt, Rinehart and Winston, 1976 (HRW international editions). https://books.google.de/books?id=1C9HAQAAIAAJ. – ISBN 9780030839931

[7] Gerthsen, K. ; Vogel, H.: *Physik*. Springer Berlin Heidelberg, 2013 (DUV Sozialwissenschaft). https://books.google.de/books?id=SbjPBgAAQBAJ. – ISBN 9783642878398

[8] Rohrer, G.S.: *Structure and Bonding in Crystalline Materials*. Cambridge University Press, 2001 https://books.google.de/books?id=a0jPqKw2Zx8C. – ISBN 9780521663793

[9] Chandrasekhar, P.: *Conducting Polymers, Fundamentals and Applications: A Practical Approach*. Springer US, 2013 https://books.google.de/books?id=Hl7mBwAAQBAJ. – ISBN 9781461552451

[10] Nalwa, H.S.: *Handbook of Advanced Electronic and Photonic Materials and Devices: Semiconductors. Vol. 1*. 2001 https://books.google.de/books?id=a9s4Wrl-014C. – ISBN 9780125137454

[11] Su, W. P. ; Schrieffer, J. R. ; Heeger, A. J.: Soliton excitations in polyacetylene. In: *Phys. Rev. B* 22 (1980), Aug, 2099–2111. http://dx.doi.org/10.1103/PhysRevB.22.2099. – DOI 10.1103/PhysRevB.22.2099

[12] Heeger, A. J. ; Kivelson, S. ; Schrieffer, J. R. ; Su, W. P.: Solitons in conducting polymers. In: *Rev. Mod. Phys.* 60 (1988), Jul, 781–850. http://dx.doi.org/10.1103/RevModPhys.60.781. – DOI 10.1103/RevModPhys.60.781

[13] Su, W. P. ; Schrieffer, J. R. ; Heeger, A. J.: Solitons in Polyacetylene. In: *Phys. Rev. Lett.* 42 (1979), Jun, 1698–1701. http://dx.doi.org/10.1103/PhysRevLett.42.1698. – DOI 10.1103/PhysRevLett.42.1698

[14] Kertesz, Miklos ; Choi, Cheol H. ; Yang, Shujiang: Conjugated Polymers and Aromaticity. In: *Chemical Reviews* 105 (2005), Nr. 10, 3448-3481. http://dx.doi.org/10.1021/cr990357p. – DOI 10.1021/cr990357p. – PMID: 16218558

[15] Jiang, De en ; Chen, Xing-Qiu ; Luo, Weidong ; Shelton, William A.: From trans-polyacetylene to zigzag-edged graphene nanoribbons. In: *Chemical Physics Letters* 483 (2009), Nr. 1, 120 - 123. http://dx.doi.org/http://dx.doi.org/10.1016/j.cplett.2009.10.061. – DOI http://dx.doi.org/10.1016/j.cplett.2009.10.061. – ISSN 0009–2614

[16] Ramasubramaniam, Ashwin ; Naveh, Doron ; Towe, Elias: Tunable band gaps in bilayer transition-metal dichalcogenides. In: *Phys. Rev. B* 84 (2011), Nov, 205325. http://dx.doi.org/10.1103/PhysRevB.84.205325. – DOI 10.1103/PhysRevB.84.205325

4 Appendix

4.1 Calculations

Calculate creation and annihilation operator in k-space (symmetric normation factors):

$$c_{2n} = \frac{1}{\sqrt{N_d}} \sum_k \exp[ik(2n)a] \cdot c_k^{(e)} \tag{4.1}$$

$$c_{2n+1} = \frac{1}{\sqrt{N_d}} \sum_k \exp[ik(2n+1)a] \cdot c_k^{(o)} \tag{4.2}$$

$$c_k^{(e)} = \frac{1}{\sqrt{N_d}} \sum_n \exp[-ik(2n)a] \cdot c_{2n} \tag{4.3}$$

$$c_k^{(o)} = \frac{1}{\sqrt{N_d}} \sum_n \exp[-ik(2n+1)a] \cdot c_{2n+1} \tag{4.4}$$

Remember: operators $c_{2n(+1)}$ operate on double unit cell length $\rightarrow$ halve Brillouin zone $\left(-\frac{\pi}{2a}, \frac{\pi}{2a}\right]$
boundary condition: $\exp[2ik(n+N_d)a] = 1 \rightarrow N_d$ allowed kpts in Brillouin zone
Check for c_{2n}:

$$c_{2n_0}(c_k^{(e)}(c_{2n_i})) = c_{2n} \tag{4.5}$$

$$= \frac{1}{\sqrt{N_d}} \sum_k \exp[ik(2n_0)a] \cdot \frac{1}{\sqrt{N_d}} \sum_n \exp[-ik(2n)a] \cdot c_{2n} \tag{4.6}$$

$$= \frac{1}{N_d} \sum_{k,n} \exp[ika(2n_0 - 2n)] \cdot c_{2n} \tag{4.7}$$

$$= \frac{1}{N_d} \sum_n N_d \delta_{2n_0,2n} c_{2n} \tag{4.8}$$

$$= c_{2n_0} \tag{4.9}$$

Warm up calculation:

$$\sum_{n}^{N_d} c_{2n+1}^{\dagger} c_{2n} = \sum_{n,k,k'} \exp[ika(2n)] \cdot \exp[-ik'a(2n+1)] \cdot \frac{c_{k'}^{\dagger(o)} c_{k}^{(e)}}{N_d} \tag{4.10}$$

$$= \sum_{n,k,k'} \exp[ia(k-k')(2n)] \cdot \exp(-ik'a) \cdot \frac{c_{k'}^{\dagger(o)} c_{k}^{(e)}}{N_d} \tag{4.11}$$

$$= \sum_{k,k'} \delta_{k,k'} \cdot \exp(-ik'a) \cdot c_{k'}^{\dagger(o)} c_{k}^{(e)} \tag{4.12}$$

$$= \sum_{k'} \exp(-ik'a) \cdot c_{k'}^{\dagger(o)} c_{k'}^{(e)} \tag{4.13}$$

Analogously:

$$\sum_{n}^{N_d} c_{2n}^{\dagger} c_{2n+1} = \sum_{k'} \exp(ik'a) \cdot c_{k'}^{\dagger(e)} c_{k'}^{(o)} \tag{4.14}$$

$$\sum_{n}^{N_d} c_{2n}^{\dagger} c_{2n-1} = \sum_{k'} \exp(-ik'a) \cdot c_{k'}^{\dagger(e)} c_{k'}^{(o)} \tag{4.15}$$

$$\sum_{n}^{N_d} c_{2n-1}^{\dagger} c_{2n} = \sum_{k'} \exp(ik'a) \cdot c_{k'}^{\dagger(o)} c_{k'}^{(e)} \tag{4.16}$$

Thus one obtains:

$$\mathcal{H} = -2 \sum_{n}^{N_d} \Big[(t_0 + \delta) \Big(c_{2n+1}^{\dagger} c_{2n} + c_{2n}^{\dagger} c_{2n+1} \Big) + (t_0 - \delta) \Big(c_{2n+2}^{\dagger} c_{2n+1} + c_{2n+1}^{\dagger} c_{2n+2} \Big) \Big] + 2N\kappa u^2 \tag{4.17}$$

$$= -2 \sum_{k'} \Big[(t_0 + \delta) \Big(\exp(-ik'a) \cdot c_{k'}^{\dagger(o)} c_{k'}^{(e)} + \exp(ik'a) \cdot c_{k'}^{\dagger(e)} c_{k'}^{(o)} \Big) + (t_0 - \delta) \Big(\exp(-ik'a) \cdot c_{k'}^{\dagger(e)} c_{k'}^{(o)} + \exp(ik'a) \cdot c_{k'}^{\dagger(o)} c_{k'}^{(e)} \Big) \Big] + 2N\kappa u^2 \tag{4.18}$$

$$= -2 \sum_{k'} \Big\{ [2t_0 \cos(k'a) + 2i\delta \sin(k'a)] c_{k'}^{\dagger(e)} c_{k'}^{(o)} + [2t_0 \cos(k'a) - 2i\delta \sin(k'a)] c_{k'}^{\dagger(o)} c_{k'}^{(e)} \Big\} + 2N\kappa u^2 \tag{4.19}$$

$$\neq -2 \sum_{k'} \Big\{ [-2t_0 \cos(k'a) + 2i\delta \sin(k'a)] c_{k'}^{\dagger(e)} c_{k'}^{(o)} + [-2t_0 \cos(k'a) - 2i\delta \sin(k'a)] c_{k'}^{\dagger(o)} c_{k'}^{(e)} \Big\} + 2N\kappa u^2 \tag{4.20}$$

Substituting $\epsilon_k := 2t_0 \cos(ka)$ and $\Delta_k := 2\delta \sin(ka)$ the following form of the hopping term can be derived:

$$\mathcal{H}_{\text{hopp},k} = [\epsilon_k + i\Delta_k] c_k^{\dagger(e)} c_k^{(o)} + [\epsilon_k - i\Delta_k] c_k^{\dagger(o)} c_k^{(e)} \tag{4.21}$$

Using this the ground state energy can be derived as follows (completely occupied valence, empty conduction band):

$$E_0(u) = -2\sum_k |E_k| + 2N\kappa u^2 \tag{4.22}$$

$$= -2\sum_k \sqrt{\epsilon_k^2 + \Delta_k^2} + 2N\kappa u^2 \tag{4.23}$$

$$= -2\sum_k \sqrt{\left[2t_0\cos(ka)\right]^2 + \left[2\delta\sin(ka)\right]^2} + 2N\kappa u^2 \tag{4.24}$$

$$\tag{4.25}$$

In the limit of $N \to \infty$ the sum becomes an integral:

$$E_0(u) = \frac{-N}{\pi}\int_{-\pi/2a}^{\pi/2a} \mathrm{d}k\ \sqrt{\left[2t_0\cos(ka)\right]^2 + \left[2\delta\sin(ka)\right]^2} + 2N\kappa u^2 \tag{4.26}$$

$$= \frac{-4Nt_0}{\pi}\underbrace{\int_0^{\pi/2} \mathrm{d}\theta\ \sqrt{1 - \left(1 - \frac{\delta^2}{t_0^2}\right)\sin^2(\theta)}}_{=:F(\delta/t_0)} + 2N\kappa u^2 \tag{4.27}$$

For small δ/t_0 the integral can be approximated as follows:

$$F\left(\frac{\delta}{t_0}\right) \approx 1 + \frac{1}{2}\left[\ln\left(\frac{4|t_0|}{|\delta|}\right) - \frac{1}{2}\right]\frac{\delta^2}{t_0^2} \tag{4.28}$$

To calculate the energies in manually charged states (cdft), use the states:

$$\Psi_k^{(v)}(q) = \sqrt{\frac{1}{2} - \frac{q}{2}}\, c_k^{\dagger(e)} - \sqrt{\frac{1}{2} + \frac{q}{2}}\,\frac{\epsilon_k - i\Delta_k}{|E_k|} c_k^{\dagger(o)} \tag{4.29}$$

To test for the correct properties one calculates $\left|\left\langle c_k^{(*)} | \Psi_k^{(v)}(q)\right\rangle\right|^2$, for example:

$$\left|\left\langle c_k^{\dagger(e)} | \Psi_k^{(v)}(q)\right\rangle\right|^2 = \left| c_k^{(e)}\left(\sqrt{\frac{1}{2} - \frac{q}{2}}\, c_k^{\dagger(e)} - \sqrt{\frac{1}{2} + \frac{q}{2}}\,\frac{\epsilon_k - i\Delta_k}{|E_k|} c_k^{\dagger(o)}\right)\right|^2 \tag{4.30}$$

$$= \frac{1-q}{2} \tag{4.31}$$

Because of the two different spin orientations of the electron an additional factor 2 has to be taken into account to get the correct number of valence electrons at the even/odd positions. Therefore the number of valence electrons is given by $1 \pm q$. The energies for this states are given

by:

$$\begin{aligned}
\left\langle \Psi_k^{(v)}(q)\right|\mathcal{H}_{\mathrm{hopp},k}\left|\Psi_k^{(v)}(q)\right\rangle &= \left[\sqrt{\frac{1-q}{2}}\,c_k^{(e)} - \sqrt{\frac{1+q}{2}}\,\frac{\epsilon_k+i\Delta_k}{|E_k|}c_k^{(o)}\right]\cdot \\
&\quad \left[[\epsilon_k+i\Delta_k]c_k^{\dagger(e)}c_k^{(o)} + [\epsilon_k-i\Delta_k]c_k^{\dagger(o)}c_k^{(e)}\right]\cdot \\
&\quad \left[\sqrt{\frac{1-q}{2}}\,c_k^{\dagger(e)} - \sqrt{\frac{1+q}{2}}\,\frac{\epsilon_k-i\Delta_k}{|E_k|}c_k^{\dagger(o)}\right] \qquad (4.32)\\
&= -\sqrt{\frac{1-q}{2}}\,c_k^{(e)}[\epsilon_k+i\Delta_k]c_k^{\dagger(e)}c_k^{(o)}\sqrt{\frac{1+q}{2}}\,\frac{\epsilon_k-i\Delta_k}{|E_k|}c_k^{\dagger(o)} \\
&\quad -\sqrt{\frac{1+q}{2}}\,\frac{\epsilon_k+i\Delta_k}{|E_k|}c_k^{(o)}[\epsilon_k-i\Delta_k]c_k^{\dagger(o)}c_k^{(e)}\sqrt{\frac{1-q}{2}}\,c_k^{\dagger(e)} \qquad (4.33)\\
&= -\sqrt{\frac{1+q}{2}}\sqrt{\frac{1-q}{2}}\left[\frac{(\epsilon_k-i\Delta_k)(\epsilon_k+i\Delta_k)}{|E_k|} + \frac{(\epsilon_k-i\Delta_k)(\epsilon_k+i\Delta_k)}{|E_k|}\right] \qquad (4.34)\\
&= -\sqrt{1-q^2}\,|E_k| \qquad (4.35)
\end{aligned}$$

For this reason the expected ground state energy as a function of the transferred charge in respect of a negligible small phonon coupling constant δ has the form:

$$E_0(q,u) = -\frac{4Nt_0}{\pi}\sqrt{1-q^2} + 2N\kappa u^2 \qquad (4.36)$$

Fit this function with simulation results for small q, see fig. 4.1. Optimized fit coefficient:

$$t_0 = 9,4\,\mathrm{eV} \qquad \text{from fit} \qquad (4.37)$$

$$t_0 = 2.5\,\mathrm{eV} \qquad \text{Glen paper} \qquad (4.38)$$

Probably this assumption is wrong:

$$\Psi_k^{(v)}(q) = \sqrt{\frac{1-q}{2}}\,c_k^{\dagger(e)} - \sqrt{\frac{1+q}{2}}\,\frac{\epsilon_k-i\Delta_k}{|E_k|}c_k^{\dagger(o)} \qquad (4.39)$$

and should rather be formulated in a more general way:

$$\Psi_k^{(v)}(q_k) = \sqrt{\frac{1-q_k}{2}}\,c_k^{\dagger(e)} - \sqrt{\frac{1+q_k}{2}}\,\frac{\epsilon_k-i\Delta_k}{|E_k|}c_k^{\dagger(o)} \qquad (4.40)$$

$$\Rightarrow \qquad \left\langle \Psi_k^{(v)}(q_k)\right|\mathcal{H}_{\mathrm{hopp},k}\left|\Psi_k^{(v)}(q_k)\right\rangle = -\sqrt{1-q_k^2}\,|E_k| \qquad (4.41)$$

With this states one can easily calculate the number of valence electrons at the even/odd posi-

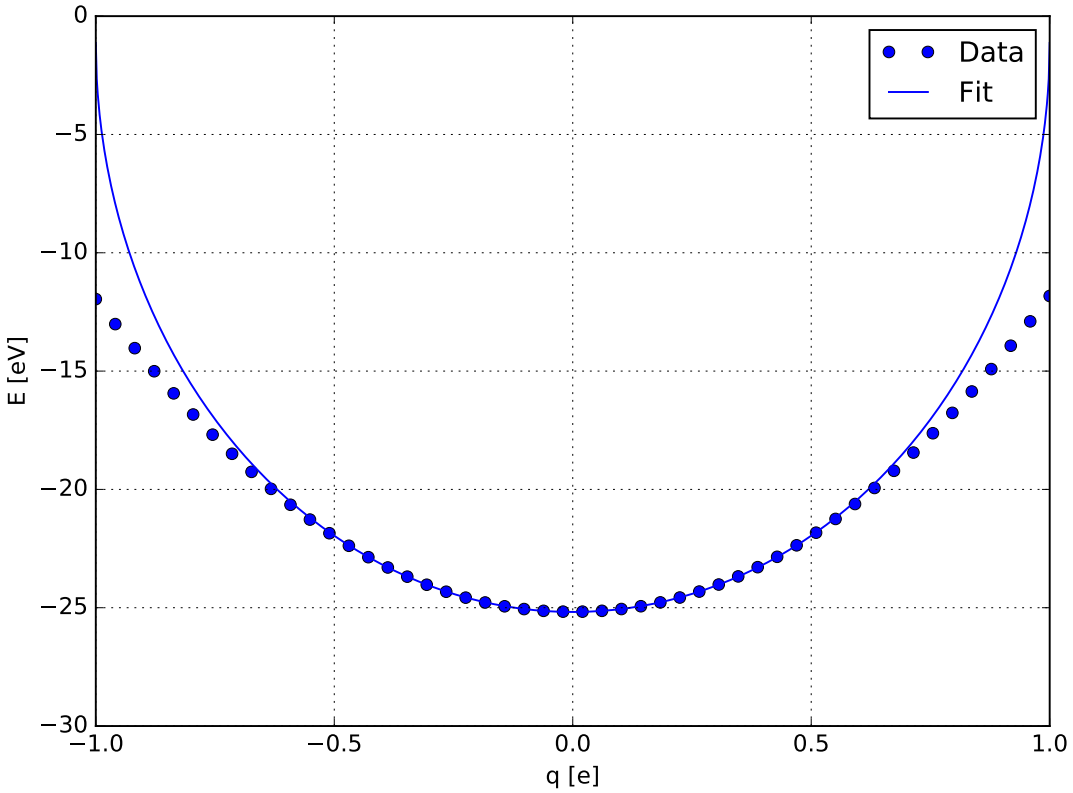

Figure 4.1: Unit cell energy as function of the manually shiftet charge for many k-points

tions, for example :

$$q_k = \vec{\Psi}_k^{*\top} \cdot \begin{pmatrix} 1 & 0 \\ 0 & 0 \end{pmatrix} \cdot \vec{\Psi}_k \tag{4.42}$$

$$= \left[2\left(E_k^2 \mp V|E_k|\right)\right]^{-1} \cdot (-V \pm |E_k|)^2 \tag{4.43}$$

$$= \frac{(-V \pm |E_k|)^2}{2(E_k^2 \mp V|E_k|)} \tag{4.44}$$

Then the ground state energy can be calculated as follows:

$$E_0 = -2\sum_k |E_k| + 2N\kappa u^2 \tag{4.45}$$

$$= -2\sum_k \sqrt{V^2 + \epsilon_k^2 + \Delta_k^2} + 2N\kappa u^2 \tag{4.46}$$

$$= -2\sum_k \sqrt{V^2 + 4t_0^2\cos^2(ka) + 4\delta^2\sin^2(ka)} + 2N\kappa u^2 \tag{4.47}$$

$$= -4t_0\sum_k \sqrt{\frac{V^2}{4t_0^2} + 1 - \left(1 - \frac{\delta^2}{t_0^2}\right)\sin^2(ka)} + 2N\kappa u^2 \tag{4.48}$$

$$= -4t_0\sqrt{\frac{V^2}{4t_0^2} + 1}\sum_k \sqrt{1 - \frac{4t_0^2 - 4\delta^2}{V^2 + 4t_0^2}\sin^2(ka)} + 2N\kappa u^2 \tag{4.49}$$

$$= -4t_0\sqrt{\frac{V^2}{4t_0^2} + 1}\sum_k \sqrt{1 - c^2 \cdot \sin^2(ka)} + 2N\kappa u^2 \tag{4.50}$$

with $c^2 = \frac{4t_0^2 - 4\delta^2}{V^2 + 4t_0^2}$. In the limit of $N \to \infty$ the sum can be transformed into an integral:

$$E_0 = \frac{-2N}{\pi}\sqrt{V^2 + 4t_0^2}\int_0^{\pi/2} \mathrm{d}\theta \sqrt{1 - c^2 \cdot \sin^2(\theta)} \tag{4.51}$$

$$= \frac{-2N}{\pi}\sqrt{V^2 + 4t_0^2} \cdot F(\sqrt{1 - c^2}) \tag{4.52}$$

To write this expression as a function of the displaced charge a relationship between the potential

V and q is needed:

$$q = \frac{2}{N}\sum_k q_k \tag{4.53}$$

$$= \langle q_k \rangle \tag{4.54}$$

$$= \left\langle \frac{(V+|E_k|)^2}{2(E_k^2+V|E_k|)} \right\rangle \tag{4.55}$$

$$= \frac{1}{2}\left(\left\langle \frac{E_k^2+VE_k}{E_k^2+VE_k} \right\rangle + V\left\langle \frac{1}{E_k} \right\rangle \right) \tag{4.56}$$

$$= \frac{1}{2}\left(1 + V\left\langle \frac{1}{E_k} \right\rangle \right) \tag{4.57}$$